JMEPEG (1995) 4:291-300

Development of a New Model for Plane Strain Bending and Springback Analysis

Z.T. Zhang and D. Lee

A new mathematical model is presented for plane strain bending and springback analysis in sheet metal forming. This model combines effects associated with bending and stretching, considers stress and strain distributions and different thickness variations in the thickness direction, and takes force equilibrium into account. An elastic-plastic material model and Hill's nonquadratic yield function are incorporated in the model. The model is used to obtain force, bending moment, and springback curvature. A typical two-dimensional draw bending part is divided into five regions along the strip, and the forces and moments acting on each region and the deformation history of each region are examined. Three different methods are applied to the two-dimensional draw bending problems: the first using the new model, the second using the new model but also including a kinematic directional hardening material model to consider the bending and unbending deformation in the wall, and the third using membrane theory plus bending strain. Results from these methods, including those from the recent benchmark program, are compared.

Keywords
bending, springback, sheet forming, mathematical modeling

1. Introduction

DIFFERENT approaches are used in the analysis of sheet metal stretch forming depending on if the bending effect is considered, whereas pure bending is often analyzed without considering stretching and force equilibrium. Finite element analysis using solid type elements (Ref 1-3) can take bending effect into account. However, the computing time is usually long, and convergence is often a problem. Finite element analysis using the shell theory (Ref 4-6) takes bending effect into account by adding a correcting term to the strain before the equilibrium equations are solved. This single correcting term may not be accurate because the thickness of the convex side usually becomes thinner due to tensile strain, and the thickness of the concave side becomes thicker due to compressive strain. Finite element analysis using membrane theory (Ref 7, 8) calculates membrane strain and bending strain separately and then combines these data. This method may not be accurate either because the effect due to bending strain is not taken into account in the equilibrium equations, and the thickness variation in the stretching and compressing areas is not considered.

The semianalytical method presented by Brunet (Ref 9) examines the details of material models, but the thickness variation is not considered. Other analytical or semianalytical methods (Ref 10-14) often provide a faster estimation of strain distribution and other parameters, but the thickness variation calculation in these methods is either inaccurate or completely neglected.

Z.T. Zhang* and **D. Lee,** Design and Manufacturing Institute and Mechanical Engineering Department, Rensselaer Polytechnic Institute, Troy, NY 12180, USA.
*University of Michigan, Dept. of Mechanical Engineering and Applied Mechanics, Ann Arbor, Mi 48109, USA.

Nomenclature

d_1	A factor, defined in Eq 14
E	Young's modulus, N/mm^2
F	Stretching force, N
F_b	Stretching force at the outer boundary, N
F_c	Stretching force at the center, N
F_w	Stretching force in the wall, N
K	Strength coefficient, N/mm^2
L_o	Initial blank length, mm
m	The exponent in Hill's anisotropy yield function
M	Bending moment, Nmm
n	Strain hardening index
r	Plastic anisotropy, plastic strain ratio
R	Bending radius of an arbitrary fiber, mm
R_i	Inner bending radius, mm
R_o	Outer bending radius, mm
R_{mo}	Original middle surface bending radius, mm
t_o	Initial blank thickness, mm
z_o	Coordinate in the thickness direction before deformation, mm
α	Bending angle
β	The ratio of bending radius to blank thickness
ΔK	Springback curvature, 1/mm
Δ_t	Thickness difference between the stretching side and the compressive side under pure bending, mm
ε	True strain
ε_o	Material constant, initial strain
$\underline{\varepsilon}_{1mo}$	True strain at the original middle surface
$\bar{\varepsilon}$	Effective strain
θ	Sheet wrapping angle around the punch corner or the die corner
μ_d	Friction coefficient between the blank and the die
μ_p	Friction coefficient between the blank and the punch
ν	Poisson's ratio
σ	True stress, N/mm^2
$\underline{\sigma}_Y$	Yield stress, N/mm^2
$\bar{\sigma}$	Effect stress, N/mm^2
Subscripts:	
1	Strip direction
2	Transverse direction
3	Thickness direction

Springback in sheet metal forming always adversely affects its final shape. It is necessary to either reduce the amount of springback by appropriate processing or to compensate for the expected springback by using a different design procedure. In

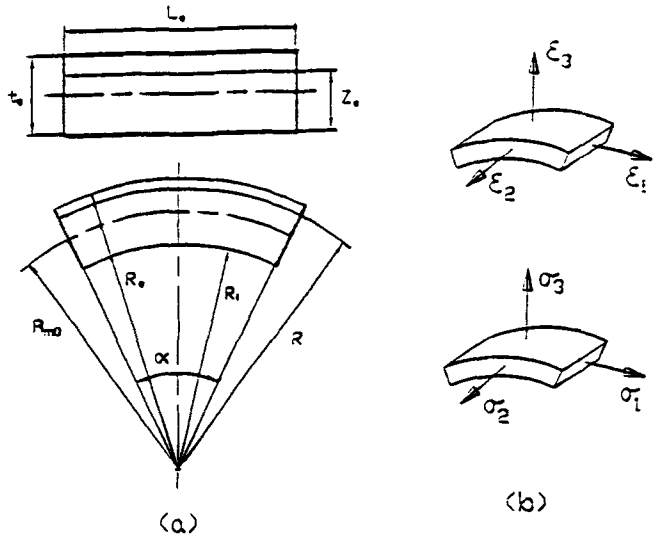

Fig. 1 Plane bending: (a) Cross sections before and after deformation; (b) Stresses and strains in plane strain bending ($\varepsilon_2 = 0$ and $\sigma_3 = 0$).

order to achieve either of these objectives, one must be able to predict accurately the magnitude of springback for a given loading method and component. The calculation of springback is based on the theorem that the distortion, or springback, caused by the unloading of a force or moment is equal to the deformation caused by the loading of a force or moment of the same magnitude but opposite direction. Therefore, the accuracy of the springback calculation depends on the accuracy of the force or moment calculation, as well as the accuracy of the moment of inertia calculation.

Based on these considerations, a new model is presented in which stretching, bending, force equilibrium, and thickness variation are incorporated at the same time. The calculation of strain, stress, force, bending moment, and moment of inertia are all based on the deformed geometry, and the error due to inaccurate geometry description is therefore eliminated.

Three methods are outlined to analyze the two-dimensional draw bending problems. Method 1 uses the new model presented in section 2. Method 2 not only uses the new model, but also adopts a kinematic directional hardening material model to reflect the bending and unbending deformation in the wall region. Method 3 uses membrane theory to account for force equilibrium, then bending strain is added to the total strain, as described by Nie et al. (Ref 14). A comparison of the results from different methods is also presented.

2. A New Model

2.1 *Bending and Stretching Strain Calculation*

In the analysis of sheet metal bending, the cross section of the bending sheet is often divided into different deformation areas. The most detailed analyses may be those given by Dadras et al. and Verguts et al. (Ref 12, 15) where the cross section was divided into three areas: stretching, compressing, and strain reversal areas. In the Dadras analysis (Ref 12), the strain reversal area was further divided into a tensile stress and strain area and an area of tensile stress but of total compression strain. In this paper, the cross section is not divided into separated areas. Stress calculation is based on the true strain involved in each fiber across the thickness.

Consider the plane strain bending and stretching deformation shown in Fig. 1(a). A flat sheet of thickness, t_o, and length, L_o, is deformed to a curved sheet with inner radius of R_i and outer radius of R_o. The radius of the original middle surface is R_{mo}. Assume that the plane cross sections remain plane and perpendicular to the deformed middle surface and the volume remains unchanged after plastic deformation whereas the volume variation due to elastic deformation is neglected. Given this, the cross-sectional area will also remain unchanged because of plane strain deformation. Under these assumptions, the area beneath an arbitrary location, z_o, before and after deformation is related by the following equation:

$$L_o z_o = \frac{\alpha}{2}(R^2 - R_i^2) \qquad \text{(Eq1)}$$

The tangential strain of the fiber at arbitrary location z_o, which is at radius R after deformation, is:

$$\varepsilon_1 = \ln \frac{\alpha R}{L_o} \qquad \text{(Eq 2)}$$

or:

$$\alpha = \frac{L_o}{R} e^{\varepsilon_1} \qquad \text{(Eq 3)}$$

Substitute Eq 3 into Eq 1:

$$z_o = \frac{e^{\varepsilon_1}}{2R}(R^2 - R_i^2) \qquad \text{(Eq 4)}$$

R can be solved from Eq 4:

$$R = \frac{z_o + \sqrt{z_o^2 + R_i^2 e^{2\varepsilon_1}}}{e^{\varepsilon_1}} \qquad \text{(Eq 5)}$$

For the original middle surface, $z_o = \frac{t_o}{2}$ and $\varepsilon_1 = \varepsilon_{1mo}$, the corresponding radius is:

$$R_{mo} = \frac{t_o + \sqrt{t_o^2 + 4R_i^2 e^{2\varepsilon_{1mo}}}}{2e^{\varepsilon_{1mo}}} \qquad \text{(Eq 6)}$$

The tangential strain of the fiber of the original middle surface is:

$$\varepsilon_{1mo} = \ln \frac{\alpha R_{mo}}{L_o} \qquad \text{(Eq 7)}$$

It is possible to express the tangential strain at arbitrary radius R as the function of the radius and tangential strain of the original middle surface according to Eq 2 and 7:

$$\varepsilon_1 = \ln \frac{R}{R_{mo}} e^{\varepsilon_{1mo}} \quad \text{(Eq 8)}$$

From Eq 8,

$$R = R_{mo}\, e^{\varepsilon_1}\, e^{-\varepsilon_{1mo}} \quad \text{(Eq 9)}$$

Substituting Eq 9 into Eq 5:

$$R_{mo} e^{\varepsilon_1}\, e^{-\varepsilon_{1mo}} = \frac{z_o + \sqrt{z_o^2 + R_i^2\, e^{2\varepsilon_1}}}{e^{\varepsilon_1}} \quad \text{(Eq 10)}$$

Strain ε_1 can be solved from Eq 10:

$$\varepsilon_1 = \frac{1}{2} \ln \frac{R_i^2\, e^{2\varepsilon_{1mo}} + 2z_o\, R_{mo}\, e^{\varepsilon_{1mo}}}{R_{mo}^2} \quad \text{(Eq 11)}$$

Substituting Eq 6 into Eq 11, the tangential strain can be expressed as the function of the original location z_o, the tangential strain of the original middle surface, and the corner radius of the punch or die:

$$\varepsilon_1(z_o,\varepsilon_{1mo},R_i) = \frac{1}{2} \frac{t_o + \sqrt{t_o^2 + 4R_i^2\, e^{2\varepsilon_{1mo}}}}{2e^{\varepsilon_{1mo}}} \frac{e^{\varepsilon_{1mo}}}{\left(\dfrac{t_o + \sqrt{t_o^2 + 4R_i^2\, e^{2\varepsilon_{1mo}}}}{2e^{\varepsilon_{1mo}}}\right)^2} \ln \frac{R_i^2\, e^{2\varepsilon_{1mo}} + 2z_o}{} \quad \text{(Eq12)}$$

2.2 *Constitutive Relations*

Under the general three-dimensional stress state, suppose the materials stress-strain relation takes the form:

$$\bar{\sigma} = \begin{cases} E\bar{\varepsilon} & \text{in elastic regions} \\ K(\varepsilon_o + \bar{\varepsilon})^n & \text{in plastic regions} \end{cases} \quad \text{(Eq 13)}$$

For plane strain and plane stress in bending as shown in Fig. 1(b), using Hill's nonquadratic yield function (Ref 16) for normal anisotropic materials, the relationship between ε_1 and σ_1 can be found:

$$\sigma_1 = Kd_1(\varepsilon_o + d_1|\varepsilon_1|)^n \quad \text{(Eq 14)}$$

in plastic regions, where

$$d_1 = \frac{1}{2}[2(1+r)]^{\frac{1}{m}}[1+2r)^{-1m-1}]^{\frac{m-1}{m}}$$

It can be shown that:

$$\sigma_1 = \frac{E}{1-\nu^2}\varepsilon_1 \quad \text{(Eq 15)}$$

If a stress-strain ($\bar{\sigma}$-$\bar{\varepsilon}$) curve is obtained from an experiment, it can be transformed into a σ_1-ε_1 curve by following equations for plastic regions:

$$\begin{cases} \sigma_1 = & \bar{\sigma} d_1 \\ \varepsilon_1 = & \bar{\varepsilon}/d_1 \end{cases} \quad \text{(Eq 16)}$$

The following equations can also be obtained for elastic regions:

$$\begin{cases} \sigma_1 = \dfrac{1}{\sqrt{1-\nu+\nu^2}}\bar{\sigma} \\ \varepsilon_1 = \dfrac{1-\nu^2}{E}\sigma_1 \end{cases} \quad \text{(Eq 17)}$$

2.3 *Calculation of Force, Bending Moment, and Moment of Inertia*

The resulting force from the stress of a unit width cross section is obtained by the following equation:

$$F = \int_{R_i}^{R_o} \sigma_1\, [\varepsilon_1\, (z_o,\varepsilon_{1mo},R_i)]\, dR(z_o) \quad \text{(Eq 18)}$$

A starting value of the original middle surface strain ε_{1mo} is initially determined. ε_1 is then calculated from Eq 12 for a specific layer of fiber with coordinate z_o in the sheet. The radius of this particular fiber is calculated from Eq 5. Equation 14 or 15 is used to find the corresponding stress depending on the deformation involved—plastic or elastic. If the stress-strain relation is given by experimental data, they are first transformed by Eq 16 and 17.

The calculated resulting force from Eq 18 is compared with the transferred force through the cross section. If the difference between the two is greater than an allowed value, the original middle surface strain is adjusted, and the above calculation procedure is repeated. This iterative process is continued until a satisfactory result is obtained.

The bending moment is calculated by:

$$M = \int_{R_i}^{R_o} \sigma_1\, (\varepsilon_1)\, [R - (R_o + R_i)/2.0] dR(z_o) \quad \text{(Eq 19)}$$

The moment of inertia is calculated by:

$$L = (R_o - R_i)^3/12 \quad \text{(Eq 20)}$$

Note that the force, the bending moment, and the moment of inertia are all calculated based on the geometry after deformation.

2.4 *Springback Calculation*

Springback refers to the change in the shape of the sheet geometry after the load has been removed. The stretching force in the sheet causes sheet shrinkage, and the bending moment causes rotation. In sheet metal forming, the shape variation caused by the bending moment is generally much larger than that caused by the stretching force, and therefore the latter is often neglected. Springback is caused by an elastic deformation, and the unloading process is normally considered as a reverse loading of the same magnitude of the loading force or bending moment, or both. Under plane strain deformation, the springback curvature caused by unloading of a bending moment is calculated by the following formula:

$$\Delta K = \frac{M(1-\nu^2)}{LE} \qquad \text{(Eq 21)}$$

The main difference of springback prediction lies in the different methods of calculating the bending moment, M. Variation of Young's modulus, E, with plastic strain has been considered according to Brunet (Ref 9), but published papers about this variation are limited.

2.5 *Thickness Variation and Pure Bending*

Most previous methods in bending analysis neglect the change of sheet thickness during deformation. Hill showed that a rigid plastic sheet cannot thin by bending alone unless tensile forces are accompanied (Ref 17). Such thickness variation after bending and its effect on the prediction of springback and other parameters are examined in this section.

Referring to Fig. 1(a), for pure bending, the original middle surface strain ε_{1mo} is zero.

$$\frac{t}{t_o} = \frac{2R_{mo}}{\sqrt{t_o R_{mo} + R_{mo}^2} + \sqrt{R_{mo}^2 - t_o R_{mo}}} \qquad \text{(Eq 22)}$$

or

where

$$\frac{t}{t_o} = \frac{2\beta}{\sqrt{\beta^2+\beta} + \sqrt{\beta^2-\beta}} \qquad \text{(Eq 23)}$$

$$\beta = \frac{R_{mo}}{t_o}$$

Although the change is very small, the thickness does change. For example, $\beta = 3.0$, t/t_o is 1.015.

Now consider the thickness difference between the tensile area and the compression area.

$$R_o - R_{mo} = \sqrt{t_o R_{mo} + R_{mo}^2} - R_{mo} \qquad \text{(Eq 24)}$$

$$R_{mo} - R_i = R_{mo} - \sqrt{R_{mo}^2 - t_o R_{mo}} \qquad \text{(Eq 25)}$$

The thickness difference of these two areas is obtained from Eq 24 and 25:

$$\Delta t = 2R_{mo} - R_i - R_o$$
$$= 2R_{mo} - \sqrt{R_{mo}^2 - t_o R_{mo}} - \sqrt{t_o R_{mo} + R_{mo}^2} \qquad \text{(Eq 26)}$$

or:

$$\frac{\Delta t}{t_o} = 2\beta - \sqrt{\beta^2+\beta} - \sqrt{\beta^2-\beta} \qquad \text{(Eq 27)}$$

For example, $\beta=3$, $\Delta t/t_o = 0.086$, or $\Delta t/(t_o/2) = 0.172$. For pure bending when strain ε_{1mo} in the original middle surface is zero, the stretched area is about 17.2% smaller than the compressed area in this situation, which may have a significant effect on the bending moment calculation. The stress resultant in the cross section is not zero and has a negative value. Therefore, an outside compressive force in the strip direction is required in order to reach pure bending. On the other hand, if pure bending is defined as when the stress resultant in the cross section is zero, the strain ε_{1mo} of the original middle surface fiber will be positive, not zero. The thickness difference between the stretched area and the compressed area also shows that using a single thickness variation coefficient for both these two areas is inaccurate; however, this method has often been adopted by others.

In calculating the bending moment, the reference point should be at the current middle surface when the stress resultant in the cross section is not zero. If stretching is involved in a bending deformation, thickness will be reduced in the same degree as the sheet elongation. So thickness variation should be taken into account in the calculation of moment of inertia. For example, if the thickness is reduced by 10%, the moment of inertia of the cross section will be reduced by 27%.

3. Analysis of Two-Dimensional Draw Bending Processes

The bending and stretching analysis in the last section is very general. It can be used for pure bending or for deformation where both bending and stretching (or compression) are involved. The two-dimensional draw bending problems as illustrated in Fig. 2(a) are considered. Although the equilibrium formulation are the same as that given by Wenner (Ref 18), a more detailed description of the process is provided, and some important phenomena are explained. The deformation area is divided into five regions along the strip direction as shown in Fig. 2(a). The forces and bending moments acting at the end of each region are shown in Fig. 2(b to h) except the forces normal to the sheet surfaces.

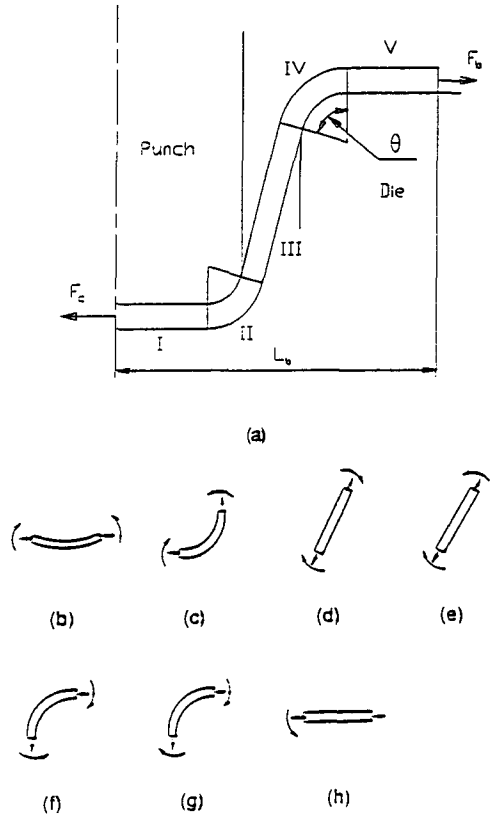

Fig. 2 (a) Deformation regions in two-dimensional draw bending processes. (b-h) Force and moment illustrations in different regions

3.1 *Region I*

This region is the flat part under the punch. Under the action of both stretching force and bending moment, the sheet will not contact the punch and should have a curvature as shown in Fig. 2(b), especially at the beginning of the forming process. This region is usually considered flat, as in membrane theory.

3.2 *Region II*

This region is the area around the punch corner and is shown in Fig. 2(c). The left area of this region is bent first and followed by subsequent stretching, whereas the right area is stretched first and followed by subsequent bending. Strictly speaking, the analysis of the left area and that of the right area of this region should be different, and the final curvature of this region after unloading will not be exactly the same. However, simplified solutions are often adopted.

3.3 *Region III*

This region is the unsupported area and may have undergone the most complex deformation in the process. In the early stage of the process, the sheet under the blank cannot move because of friction. The forces and moments acting on this region are shown in Fig. 2(d). Large shear stresses, which are normal to the surface and now shown, will exist at both ends of this region to balance the moments of the same direction (clockwise direction) acting on both ends. The bending moment in the cross section is positive at the lower left side and negative at the upper right side. At some point near the middle, it is zero. This is the condition of stretching. In the downward movement of the punch, part or all of this area may be bent around the punch corner, depending on the magnitude of the punch corner radius, the gap between the punch and the die, and the die corner radius.

If the stretching force in this region can overcome the fraction force from the die corner and under the blankholder or draw bead, the sheet will be drawn in and becomes part of this region. The forces and moments acting on this region under this situation are shown in Fig. 2(e). If there is no draw bead and the sheet under the blankholder only undergoes elastic deformation, the sheet in this area will have the deformation history of bending around the die corner and unbending coming out of the die corner. If the sheet under the blankholder undergoes plastic stretching, an additional stretching deformation history will have to be considered.

3.4 *Region IV*

This region is the area around the die corner. The forces acting on this region at the early stage, when there is no drawn-in and stretching deformation occurs, are shown in Fig. 2(f). With the flow of the material under the blankholder, this initial area may become part of region III, and the forces and moments acting on subsequent material in this region are shown in Fig. 2(g). If sticking occurs, then it will have the same force and moment diagram as shown in Fig. 2(f).

3.5 *Region V*

This is the region under the blankholder. The forces and moments acing on this region are shown in Fig. 2(h). In drawing a symmetric cup, the friction force under the blankholder is usually considered as acting on the edge of the sheet because of thickening. In this two-dimensional draw bending problem, if the blankholder force is not large enough to produce thinning, the friction force will act on the entire region. Otherwise, the friction force varies along the strip and decreases inwardly. It may become zero at some point before reaching region IV because the sheet becomes so thin that it loses contact with the blankholder. If there is no draw bead, the sheet in this region will remain straight after unloading.

3.6 *Sticking Problem*

Wenner has given an excellent description in this respect (Ref 18) where the friction in region V is assumed to act on the boundary, and the friction coefficient at the punch corner is assumed to be equal to that at the die corner. In that case, the force at the center and that at the boundary are equal, and sticking will occur simultaneously at both the punch corner and the die corner. Under sliding conditions, if the friction coefficient at the punch corner, μ_p, is different from the friction coefficient at the die corner, μ_d, the force at the center, F_c, will be different from the force at the boundary, F_b (refer to Fig. 2).

$$F_b = F_w e^{-\theta\mu_d} \qquad \text{(Eq 28)}$$

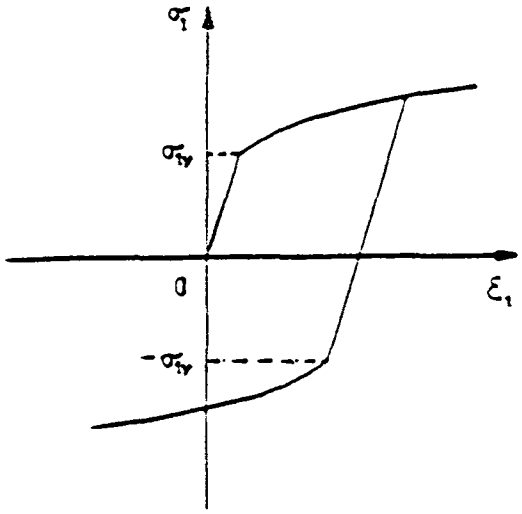

Fig. 3 Stress vs. strain in kinematic directional hardening materials

and

$$F_c = F_w e^{-\theta\mu_p} \quad \text{(Eq 29)}$$

F_w is the wall force in region III.

Differentiating F_b and F_c with respect to θ, we obtain:

$$\frac{dF_b}{d\theta} = \frac{dF_w}{d\theta} e^{-\theta\mu_d} - \mu_d F_w e^{-\theta\mu_d} \quad \text{(Eq 30)}$$

and

$$\frac{dF_c}{d\theta} = \frac{dF_w}{d\theta} e^{-\theta\mu_p} - \mu_p F_w e^{-\theta\mu_p} \quad \text{(Eq 31)}$$

When F_b or F_c Reaches its maximum value, sticking begins to occur. This requires that:

$$\frac{dF_w}{F_w d\theta} = \mu_d \quad \text{(Eq 32)}$$

or

$$\frac{dF_w}{F_w d\theta} = \mu_p \quad \text{(Eq 33)}$$

This is the critical condition. If $\mu_d > \mu_p$, and sticking does occur in the process, it occurs first on the die surface. Whether sticking occurs on the punch surface will depend on if the condition in Eq 33 can be reached in subsequent deformation. If sticking does not occur on the die surface, it will never occur on the punch surface. If $\mu_d < \mu_p$, an opposite result can be obtained with an analysis similar to that shown above.

3.7 *Three Analysis Methods*

In order to examine the new model presented previously, three methods are used in analyzing the two-dimensional draw bending problems. In all three methods, the stress resultant per unit width is calculated using Eq 18, and the applied force balance along the strip direction is considered in the same way as suggested by Wenner (Ref 18). Region I and region V are assumed as flat both before and after unloading. Region III is assumed as flat before unloading and having curvature after unloading due to springback.

Method 1 adopts the calculation procedure described in section 2 for both region II and region IV. The bending moment at the boundary between region III and region IV is considered to be equal to that of region III and is used to calculate the springback curvature of region III.

Method 2 is the same as method 1 except that a kinematic directional hardening material model, as shown in Fig. 3, is used to determine the strain, stress, force, and bending moment in region III. Unbending occurs when the sheet enters region III from region IV where it undergoes bending as well as stretching deformation. The whole region III is assumed to have undergone the same deformation history, being straight before unloading and having a constant curvature after springback.

Method 3 uses membrane theory to calculate the original middle surface strain, stress, and force for both region II and region IV. Bending strain is added to the total strain afterwards as described by Nie (Ref 19). Bending and unbending are not considered in this method.

These three methods were implemented in a computer aided bending and springback analysis system. Sample cases were examined and are presented in the next section.

4. Results

The three methods described in the last section were applied to the two-dimensional draw bending problems examined in the NUMISHEET '93 International Conference (Ref 20). The punch width is 50 mm, and the die inner width is 52 mm. The punch corner radius and die corner radius are both 5 mm. The punch displacement is 70 mm, and the friction coefficient is 0.162. The blankholder force used is 19.6 KN. The fraction force caused by the blankholder force is assumed to act at the boundary where L_b=85 mm. The material used is aluminum alloy, and its parameters are: K=570.4 N/mm^2, n=0.3469, ε_0=0.01502, E=71 GPa, ν=0.33, r=0.71, t_0=0.81 mm, σ_y=137.0 N/mm^2, and m=2 for the Hill nonquadratic yield model (Ref 16).

4.1 *Strain Distribution Predictions*

The computed strain distributions along the strip direction are shown in Fig. 4. Method 1 predicts higher membrane strain (original middle surface strain) in region II and IV than in any other areas as shown in Fig. 4(a). This may help to explain why

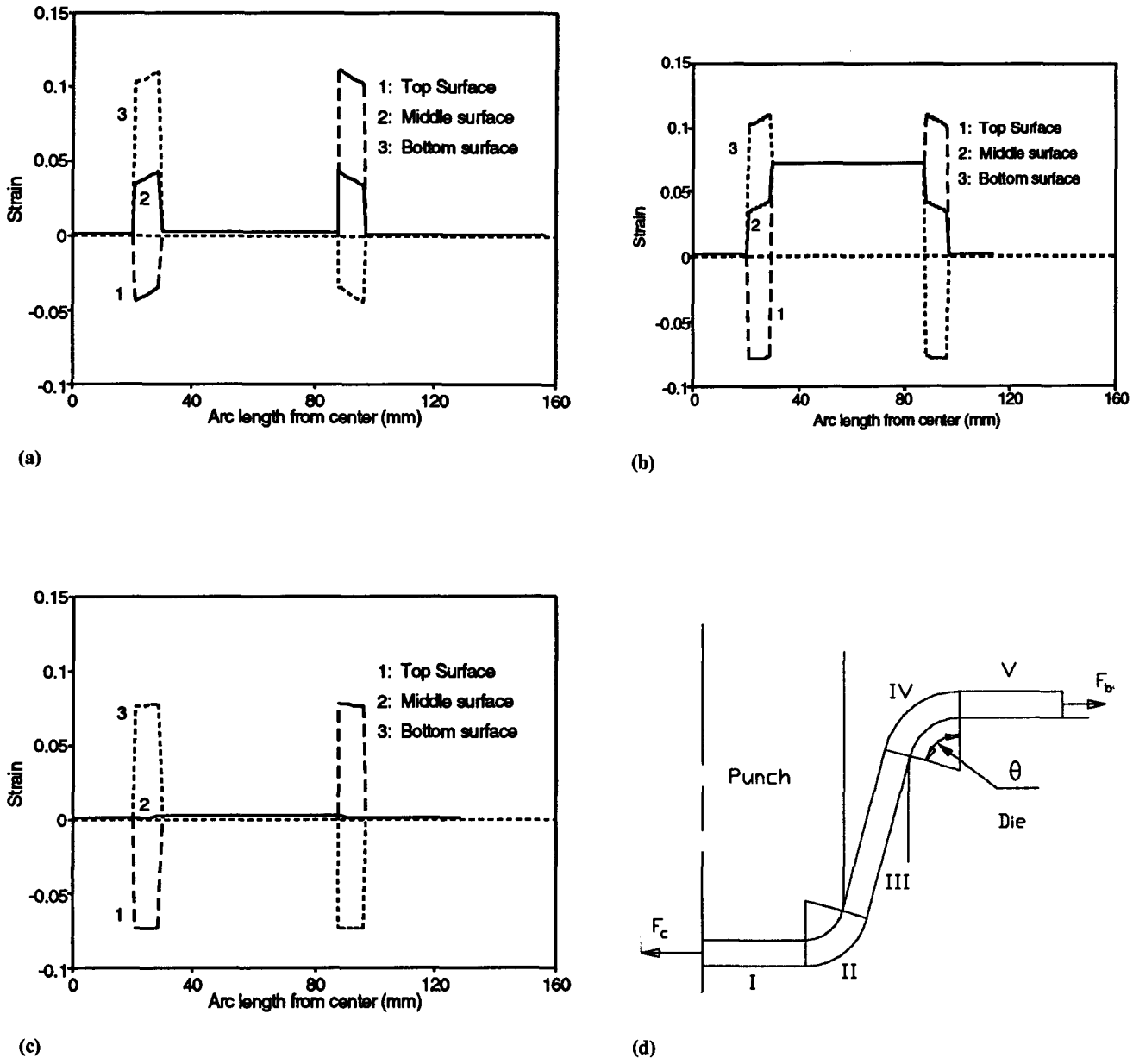

Fig. 4 Strain distributions predicted by different analysis methods: (a) method 1, (b) method 2, (c) method 3, (d) deformation regions

failure often occurs at the punch corner or the die corner if the higher surface strain on the convex side is not enough to explain this phenomena because of high strain gradient along the thickness direction. Method 2 predicts higher membrane strain in region III than in any other region, as high as the surface strain on the convex side around the corners, as shown in Fig. 4(b). Method 3 predicts almost the same magnitude of membrane strain for all areas as shown in Fig. 4(c). This may not be correct because higher membrane strain has been observed in region III than in regions I and V in experiments.

As demonstrated in section 2, membrane strain exists in the original middle surface for zero stretching force. this is examined in Fig. 5 with zero blankholder force, which results in zero stretching force. Methods 1 and 2 predict more than 0.3% membrane strain in region II and in region IV. Method 2 predicts about 0.17% membrane strain in region III when bending and unbending deformation is considered. These strains are small. But when the ratio of thickness to punch radius is increased, the membrane strain becomes larger. Method 3 predicts zero membrane strain for all regions.

4.2 *Springback Predictions*

The springback parameters defined for the two-dimensional draw bending problems in NUMISHEET '93 (Ref 20) are calculated using these three methods and compared against the experimental and simulation results presented in NUMISHEET '93 International Conference in Table 1 (Ref 20) where the results from using blankholder force of 2.45 KN and 12.0 KN are also listed.

Since springback is mainly caused by the bending moment, the bending moment distributions from different methods are shown in Fig. 6(a). In regions II and IV. methods 1 and 2 predict the same magnitude of bending moment, whereas at region III, method 2 predicts a slightly higher bending moment than method 2. Method 3 predicts the highest bending moment for all three middle regions.

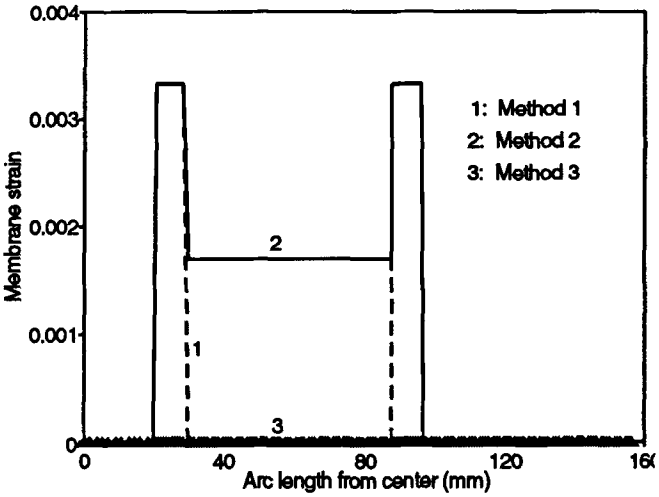

Fig. 5 Membrane strain distributions predicted by different methods under zero stretching force

Springback curvature ΔK distributions are shown in Fig. 6(b). Although the bending moments in region III predicted by methods 1 and 2 are almost the same, the springback curvature distributions predicted by them are quite different, because method 2 predicts a thinner thickness than method 1. The sign of the springback curvature is disregarded in the diagram.

The springback parameters predicted by method 1 are more consistent with the NUMISHEET experimental averages. The shapes predicted by the three methods after unloading are compared with the shape before unloading in Fig. 6(c). Method 1 gives the closest shape prediction to the NUMISHEET experimental averaged shape.

The parameters listed in Table 1 show that when blankholder force is small (2.45 KN), the differences between the springback predictions from these three methods are small. When the blankholder force is increased to 19.6 KN, their differences become larger, which are shown in Fig. 7. The variation ranges of the NUMISHEET experimental results are much smaller than those of the simulation results.

5. Comments

A new mathematical model is presented for the calculation of strain, stress, force, bending moment, and springback under a plane strain sheet metal bending and stretching condition. The new model couples bending and stretching together, considers different thickness variation along thickness direction, and takes force equilibrium into account. The model includes all of the important tool geometry and material parameters in quasi-static plane strain bending and stretching, which allows detailed parameter sensitivity analysis in these processes. In this model, it is assumed that the inner radius of a bending part is known. This can be changed to assume that the original middle surface radius is known. This model can be used in finite element analysis to calculate strain and stress where the curvature is not defined by tool geometry, thus giving more accurate results. However, the formulation of doing so would be very complicated.

Table 1 Springback results from different methods

	Methed 1	Method 2	Method 3,	NUMISHEET '93 experimental	NUMISHEET '93 simulation
Blankholder force, 2.45 KN					
θ_1, degrees	114.3	114.5	114.5	101.5 - 116.0	62 - 134
θ_2, degrees	76.0	75.8	75.6	68.0 - 77.5	63 - 91
$\theta_1 - \theta_2$, degrees	38.3	38.7	38.9		
ρ, mm	88.5	87.7	87.3	75.7 - 217.0	60 - 531
Blankholder force, 12.0 KN					
θ_1, degrees	111.8	113.4	114.5	...	...
θ_2, degrees	77.9	76.3	75.6	...	...
$\theta_1 - \theta_2$, degrees	33.9	37.1	38.9	...	...
ρ, mm	100.2	91.4	87.3	...	...
Blankholder force, 19.6 KN					
θ_1, degrees	108.0	110.6	114.5	99.0 - 115.0	72 - 127
θ_2, degrees	80.6	77.9	75.6	69.9 - 84.0	68 - 93
$\theta_1 - \theta_2$, degrees	27.4	32.7	38.9		...
ρ, mm	123.8	103.7	87.2	81.0 - 287.2	82 - 27000

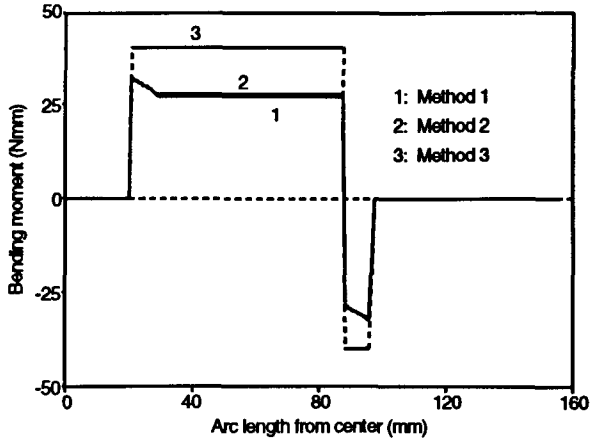

(a)

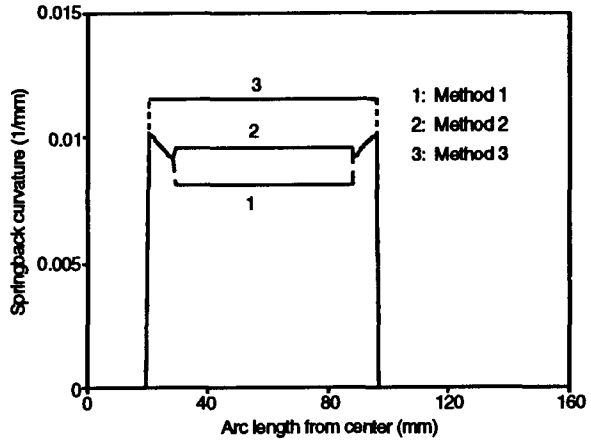

(b)

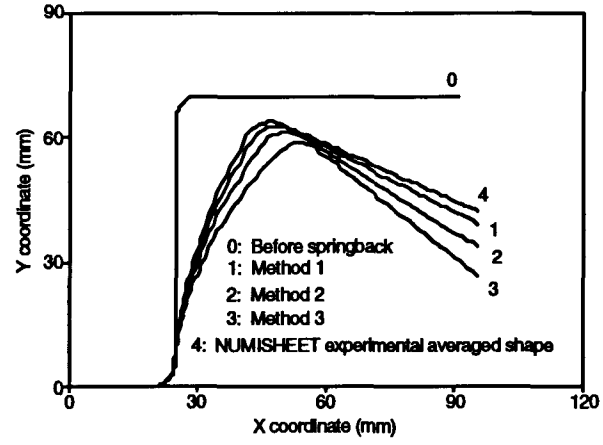

(c)

Fig. 6 Other results predicted by different methods: (a) bending moment distributions, (b) springback curvature, and (c) shape comparison before and after unloading

A compressive force is required to reach pure bending defined as the original middle surface strain being zero. On the other hand, if pure bending is defined as the stress resultant of the cross section being zero, the original middle surface will have a positive strain, or stretching strain.

A detailed analysis of the two-dimensional draw bending processes is provided. Analysis results from three different methods, as well as the results from the NUMISHEET '93 Conference, are presented for the two-dimensional draw bending problems. Method 1, using the new model and without considering bending and unbending, gives the best springback prediction among the discussed methods.

The process analysis and the results help to explain why the flat part under the punch becomes curved, why failure often occurs at the punch corner or at the die corner, why the membrane strain in the wall is so large and the curvature varies, and why the results from different analyses vary significantly.

Acknowledgments

A portion of the material reported in this paper is based upon the work supported by the National Science Foundation grant No. 8922289 and General Motors Technical Center.

References

1. A.S. Wifi, An Incremental Complete Solution of the Stretch-Forming and Deep-Drawing of a Circular Blank Using a Hemispherical Punch, *Int. J. Mech. Sci.*, Vol 18, 1976, p 23-31
2. S.I. Oh and S. Kobayashi, Finite Element Analysis of Plane Strain Sheet Metal Forming, *Int. J. Mech. Sci.*, Vol 22, 1980, p 583-594
3. B.S. Andersen, A Numerical Study of the Deep-Drawing Process, *Numerical Methods in Industrial Forming Processes*, J.F. Pittman et al., Ed., Pineridge Press, 1982, p 709-721
4. S.C. Tang, E. Chu, and S.K. Samanta, Finite Element Prediction of the Deformed Shape on an Automotive Body Panel during Preformed Stage, *Numerical Methods in Industrial Forming Processes*, J.F. Pittman et al., Ed., Pineridge Press, 1982, p 629-640
5. T.Y Tatenami, Y. Nakamura, and K. Sato, An Analysis of Deep-Drawing Process Combined with Bending, *Numerical Methods in Industrial Forming Processes*, J.F. Pittman et al., Ed., Pineridge Press, 1982, p 687-696
6. N.-M. Wang and S.C. Tang, Analysis of Bending Effects in Sheet Metal Forming Operations, *Int. J. Numer. Methods Eng.*, Vol 25, 1988, p 253-267
7. F. Pourboghrat and K. Chandorkar, Springback Calculation for Plane Strain Sheet Forming Using Finite Element Membrane Solution, *Numerical Methods for Simulation of Industrial Metal Forming Processes*, CED-Vol 5/AMD Vol 156, ASME, 1992, p 85-93
8. F. Pourboghrat and E. Chu, Prediction of Springback and Sidewall Curl in 2D-Draw Bending, *Proceedings of the 2nd International Conference of Numerical Simulation of 3-D Sheet Metal Forming Processes* (Isehara, Japan), Sheet Metal Forming Research Group, Japan,1993, p 337-351
9. M. Brunet, Benchmark Problem Solution, *Proceedings of the 2nd International Conference of Numerical Simulation of 3-D Sheet Metal Forming Processes* (Isehara, Japan), Sheet Metal Forming Research Group, Japan, 1993, p 658-659
10. H.W. Swift, Plastic Bending under Tension, *Engineering*, Vol 166, 1948, p 333-335, 357-359
11. K.A. Stelson and D.C. Gossard, An Adaptive Pressbrake Control Using an Elastic-Plastic Material Model, *J. Eng. Ind.*, Vol 104, 1982, p 389-393

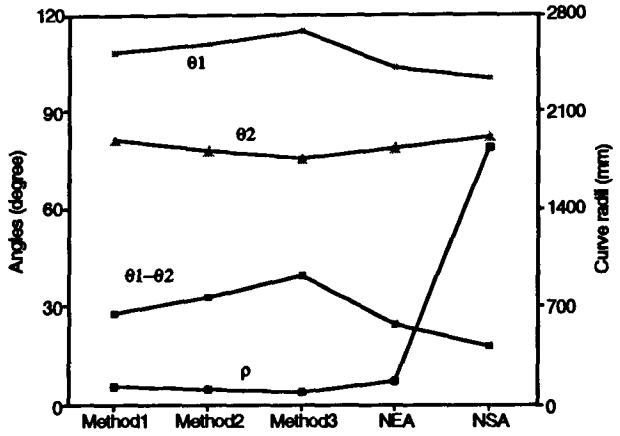

Fig. 7 Springback parameters from different methods (blank-holder force = 19.6 KN)

12. P. Dadras and S.A. Majlessi, Plastic Bending of Work Hardening Materials, *J. Eng. Ind.*, Vol 104, 1982, p 224-230
13. A. Chandra, Real Time Identification and Control of Springback in Sheet Metal Forming, *J. Eng. Ind.*, Vol 109, 1987, p 265-273
14. Q.Q. Nie and D. Lee, Comparison of Different Analytical and Experimental Results Obtained Under Simple Sheet Metal Forming Processes, *Advanced Technology of Plasticity 1993, Proceedings of the 4th International Conference on Technology of Plasticity* (Beijing),International Academic publisher, (Beijing) 1993, p 1630-1634
15. H. Verguts and R. Sowerby, The Pure Plastic Bending of Laminated Sheet Metals, *Int. J. Mech. Sci.*, Vol 17, 1975, p 31-35
16. R. Hill, Theoretical Plasticity of Textured Aggregates, *Mathematical Proceedings of Cambridge Philosophical Society*, Vol 85, 1979, p 179
17. R. Hill, *The Mathematical Theory of Plasticity*, Clarendon, 1950
18. M.L. Wenner, Elementary Solutions and Process Sensitivities for Plane Strain Sheet Metal Forming, *J. Appl. Mech.*, Vol 59, 1992, pS23-28
19. Q.Q. Nie, Finite Strain and Springback Analysis of Forming Processes with Finite and Experimental Verifications, Ph.D. thesis, Rensselaer Polytechnic Institute, 1993
20. NUMISHEET '93, Numerical Simulation of 3-D Sheet Metal Forming Processes—Verification of Simulation with Experiment, *Proceedings of the 2nd International Conference of Numerical Simulation of 3-D Sheet Metal Forming Processes* (Isehara, Japan) Sheet Metal Forming Research Group, Japan, 1993